Jurnal Teknologi

Full Paper

INFLUENCE OF MIXING AND THERMAL PARAMETERS ON THE STRUCTURAL HOMOGENEITY AND DIELECTRIC PERFORMANCE OF NBT CERAMICS

Othman N. S[a,b], Zalita Zainuddin[a], A. Atiqah[c], W H Lee[b]

[a]Department of Applied Physics, Faculty of Science and Technology, Universiti Kebangsaan Malaysia, 43600 UKM Bangi, Malaysia
[b]Universiti Kuala Lumpur, Faculty Pharmacy and Health Sciences, No. 3 Jalan Greentown, 30450 Ipoh, Perak, Malaysia
[c]Institute of Microengineering and Nanoelectronics, Universiti Kebangsaan Malaysia, 43600 UKM Bangi, Selangor, Malaysia

Article history
Received
30 April 2025
Received in revised form
4 November 2025
Accepted
17 November 2025
Published Online
16 June 2026

*Corresponding author
nurshakila@unikl.edu.my

Graphical abstract

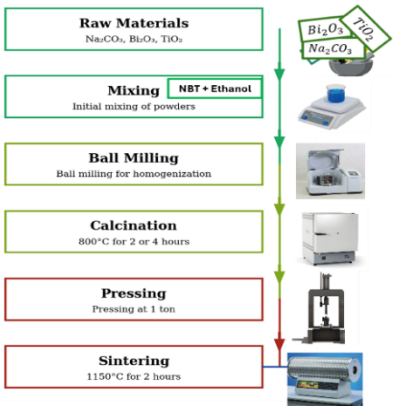

Abstract

Sodium Bismuth Titanate ($Na_{0.5}Bi_{0.5}TiO_3$, NBT) is a promising lead-free ferroelectric materials, but the role of processing parameters on its structural and dielectric performance is not well understood. This study investigates the impact of four different mixing methods: no ball milling, mixing and milling, moderate mixing and milling, and short-intensity mixing, on the properties of NBT ceramics synthesized by solid-state reaction and sintered at 1150 °C. The results show that enhanced mixing improves phase purity and structural uniformity. Notably, short-intensity mixing yields ceramics with sharp X-ray diffraction peaks of the rhombohedral R3c phase and high relative densities (73 - 91%). These features are associated with excellent dielectric properties, including high permittivity (2000 - 6000 at 1 kHz, 300 °C) and a stable Curie temperature (320 °C). This study highlights the importance of mixing conditions in optimizing the structure–property relationship of NBT ceramics and offers practical guidelines for processing high-performance lead-free ferroelectric devices.

Keywords: Sodium Bismuth Titanate (NBT), Solid state reaction method, structural, dielectric properties

Abstrak

Natrium Bismut Titanat ($Na_{0.5}Bi_{0.5}TiO_3$, NBT) ialah bahan ferroelektrik bebas plumbum yang berpotensi tinggi, namun kesan parameter pemprosesan terhadap sifat struktur dan dielektriknya masih kurang difahami. Kajian ini menyelidiki kesan empat kaedah pencampuran:tanpa pengisaran bola, pencampuran dan pengisaran, pengisaran sederhana, dan pencampuran berintensiti singkat, terhadap sifat seramik NBT yang disintesis melalui tindak balas pepejal dan disinter pada 1150 °C. Hasil kajian menunjukkan bahawa pencampuran yang lebih baik meningkatkan ketulenan fasa dan kehomogenan struktur. Kaedah pencampuran berintensiti singkat menghasilkan seramik dengan puncak sinar-X tajam bagi fasa rombohedral R3c serta ketumpatan relatif yang tinggi (73–91%). Ciri-ciri ini berkait rapat dengan sifat dielektrik yang cemerlang, termasuk permitiviti tinggi (2000–6000 pada 1 kHz, 300 °C) dan suhu Curie yang stabil (320 °C). Kajian ini menekankan kepentingan pencampuran dalam mengoptimumkan hubungan struktur-sifat seramik NBT serta menyediakan panduan praktikal bagi pemprosesan peranti ferroelektrik bebas plumbum berprestasi tinggi.

Kata kunci: Natrium Bismut Titanat (NBT), kaedah tindak balas keadaan pepejal, struktur, sifat dielektrik

1.0 INTRODUCTION

NBT has gained substantial interest as a possible lead-free ferroelectric material due to its attractive dielectric properties and environmental benefits. It behaves as a critical lead-free electronic material because its R3c space group represents a rhombohedral perovskite structure, enabling multiple ferroelectric and piezoelectric effects [32]. The worldwide interest in NBT as a lead-free alternative primarily stems from initiatives to eliminate PZT from electronics due to environmental constraints and health-related requirements [28]. There is still a need for more insight into how processing variables during mixing affect the microstructure formation and performance results of NBT. The deficit in understanding the effects of processing history on ceramic material functional behavior remains crucial because ceramic properties result mainly from their production procedures.

Recent studies have shown that optimized mixing parameters can significantly alter the nucleation and growth mechanisms of ceramic powders and therefore affect the crystallinity, grain size, and phase purity. It is well known that enhanced mixing improves the homogeneity of the precursor blend and thus reduces problems such as bismuth volatilization and secondary phase formation which can otherwise degrade the dielectric properties of NBT. Najah Rhimi *et al*. [32] reported that improved crystallinity, as indicated by sharper X-ray diffraction (XRD) peaks, is directly correlated with superior dielectric properties, including a high dielectric constant of 3871 at the Curie temperature [32]. Likewise, Mesrar *et al*. [24] noticed that the crystallinity and dielectric response are correlated for NBT. The value of the dielectric constant ranges between 3203 and 3383 at high temperatures (450°C). This suggests that the NBT-based ceramics do rely on the controlled optimal stoichiometry of their mixed elements to achieve better ceramic performance.

Pal *et al*. [28] observed that the Curie temperature of NBT at 1 kHz was 320°C, and they attributed this phase transition with an intrinsic one regardless of the different processing routes employed, even though near-peak dielectric performance is very sensitive to processing conditions [28]. This study focused on the effects of different mixing conditions on the structure and dielectric properties of NBT ceramics [44]. Based on the advanced processing methods, a full characterization structure–property relationship has been established through XRD analysis, impedance spectroscopy, as well as LCR meter measurements. The objective of the results is to provide us with the best set of distribution parameters to manufacture high properties of NBT ceramics. Therefore, this paper deals with the investigation of mixing and milling processing conditions on NBT ceramics' structure, dielectric, as well as the electrical properties.

2.0 METHODOLOGY

2.1 Materials

For this work, we used the powders prepared by solid-state reaction as described in the section on sample preparation to produce $Na_{0.5}Bi_{0.5}TiO_3$ (NBT). The stoichiometric equations used to prepare samples were:

$$Na_2CO_3 + Bi_2O_3 + 4TiO_2 \rightarrow 4(Na_{0.5}Bi_{0.5}TiO_3) + CO_2 \quad (1)$$

For the preparation of NBT ceramics, bismuth oxide (Bi_2O_3; 99.9%, Sigma-Aldrich), ultrapure sodium carbonate (Na_2CO_3; 99.9%, Sigma-Aldrich), alongside titanium dioxide (TiO_2;99.9%, Sigma-Aldrich) were used. These were the precursors of NBT ceramics. Such precursors, with the additional 2 wt% of Na_2CO_3, were calculated according to the chemical formula in Eq. (1), considering that added sodium compensates for eventual loss of it due to sodium volatilization at high-heating temperatures. The total weight of the precursor mixture used for synthesizing each NBT batch was 4.8 g for each pellet.

NBT samples were prepared at different mixing, milling, and thermal sintering parameters for the study of their influence on structural and dielectric properties. These four unique mixing scenarios were outlined in Table 1. For this experiment, the main variable was mixing, using a magnetic stirrer. Ethanol was added in a set powder-to-ethanol ratio to improve mixing and minimize agglomeration. Following the mixing process, the resultant slurries were dried at 80 °C for 2 hours to remove the ethanol. The dried powders were then subjected to ball milling (except for NBT1) for 2 hours to further reduce particle size and improve homogeneity. The powders were placed in an agate jar with zirconia balls (5 mm diameter) and milled using a high-energy planetary ball mill (Fritsch PULVERISETTE 6).

Subsequently the powders were calcined in air using a consistent heating rate of 5°C/min to facilitate phase formation and eliminate volatile components. After calcination, the powders were ground with an agate mortar and pestle to make the particles smaller and improve sintering process. The ground powders were then uniaxially pressed into disk-shaped pellets (13 mm diameter, 1 mm thickness) under a pressure of 1 ton. These green pellets were then sintered according to their respective parameters in air with a heating rate of 5°C/min, followed by natural cooling to room temperature to achieve densification and grain growth. X-ray diffraction (XRD) was used to confirm phase formation and structural features.

Table 1 Mixing and thermal parameters

Sample	Mixing Conditions	Ball Milling	Calcination Conditions	Sintering Conditions
NBT1 (No Ball Milling)	5 hours at 500 rpm	None	890°C for 4 hours	1160°C for 2 hours
NBT2 (Mixing and Milling)	5 hours at 500 rpm	2 hours	900°C for 2 hours	1160°C for 2 hours
NBT3 (Moderate Mixing and Milling)	2 hours at 250 rpm	2 hours	890°C for 4 hours	1150°C for 2 hours
NBT4 (Short-Intensity Mixing)	1 hour at 500 rpm	2 hours	851°C for 7 hours	1099°C for 2 hours

2.1 Electrical Characterization

The dielectric properties, including the real and imaginary parts of the permittivity, were measured using a precision impedance analyzer (Autolab) over a frequency range of 100 Hz to 1 MHz at room temperature. Temperature-dependent dielectric measurements were also conducted from room temperature to 700 °C using an LCR meter to identify phase transitions and evaluate the thermal stability of the dielectric response.

This method allowed a detailed study of how processing parameters affect microstructure and dielectric behaviour in NBT ceramics. It also gave useful insights for improving lead-free ferroelectric materials, as shown in Figure 1.

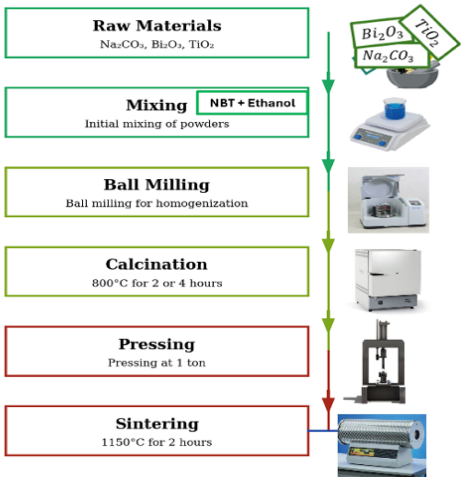

Figure 1 Synthesis process

2.2 Characterization Techniques

NBT ceramics were analyzed using an X-ray diffractometer (XRD, Advance Bruker) with CuKa radiation (λ = 1.5406 Å) to determine the crystalline structure and phase of the sintered ceramic, operating at 40 kV and 40 mA. Diffraction patterns were captured and stored within the specified 20-80° range. Subsequently, the XRD patterns were compared against patterns ICDD references 01-080-8493 and 01-074-9525 to verify that the rhombohedral NBT phase was formed and present. Only certain samples underwent Pawley refinement to quantify secondary phases and to determine lattice parameters. The bulk density of the sintered pellets was measured using a Mettler Toledo densitometer with silicon oil as the immersion medium. The density value was determined by using Archimedes' principle.

The dielectric properties of the NBT ceramics were measured using an LCR meter (model GW-Instek 819), which is connected to a computer-controlled furnace (Thermolyne F48010-33). Prior to measurement, the sintered pellets were polished to ensure parallel surfaces and coated with silver paste on both sides to serve as electrodes. The εr and tan δ were measured at a frequency of 1 kHz at temperatures ranging from 28 to 700 °C. The temperature dependence of the dielectric properties was recorded during heating at a rate of 2 °C/min. The Curie temperature (TC) was determined from the temperature corresponding to the maximum dielectric constant at 1 kHz.

3.0 RESULTS AND DISCUSSION

3.1 Effects of Mixing Parameters on Crystal Structure

The XRD patterns shown in Figure 2 indicate that all samples exhibit the rhombohedral NBT phase with space group R3c (161), consistent with the ICDD reference patterns (01-080-8493 and 01-074-9525). The lattice parameters (a = 5.499-5.501 Å, c = 13.472-13.562 Å) remain stable under different mixing and thermal conditions, demonstrating the robustness of the basic crystal structure. However, variations in peak intensities and widths among the samples suggest that the mixing and thermal parameters significantly influence crystallite size. Samples subjected to more intensive mixing exhibit stronger and sharper diffraction peaks, particularly at 2θ ≈ 32.5° (d = 2.75 Å) and 46.7° (d = 1.94 Å), indicating enhanced crystallinity. This improvement is most evident in the NBT3 sample. The crystallite size of the NBT powders was estimated using the Scherrer equation, based on the full width at half maximum (FWHM) of the main diffraction peaks. The calculated sizes for the prominent peaks at 2θ ≈ 22.8°, 32.4°, 40.1°, and 46.6° were in the range of 40.5 to 43.2 nm. This nanocrystalline scale is consistent with values reported in previous studies [36];[16], and further supports the improved crystallinity observed in intensively mixed samples. Peak indexing was performed based on the reference diffraction pattern for rhombohedral $Na_{0.5}Bi_{0.5}TiO_3$ (ICDD 01-080-8493). The main peaks at 2θ ≈ 22.8°, 32.4°, 40.1°, 46.6°, and 57.9° were assigned to the (100), (113), (024), (122), and (018) planes, respectively, confirming the formation of a single-phase rhombohedral structure with space group R3c. Among all samples, NBT3 exhibited the most intense

and sharpest diffraction peaks, indicating superior crystallinity. Combined with an intermediate crystallite size (29.55 nm), this suggests that the mixing parameters used for NBT3 synthesis were optimal (Table 2).

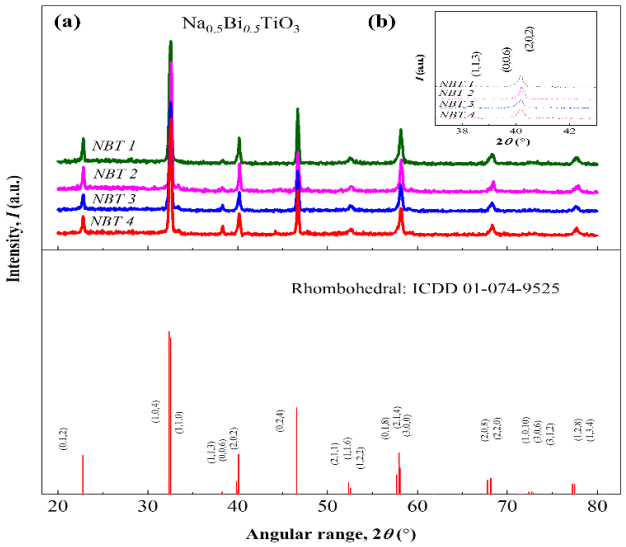

Figure 2 a) XRD diffractogram of four methods synthesizing NBT b) Small scale chosen

Table 2 Crystallite size

Sample	Crystallite size (nm)
NBT1	34.48
NBT2	34.49
NBT3	29.55
NBT4	22.51

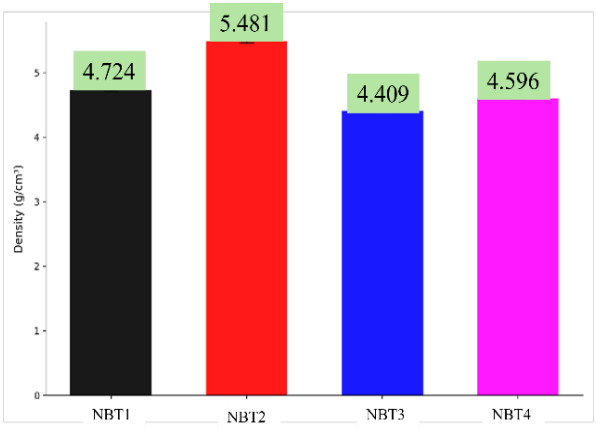

Figure 3 Densities of NBT ceramics synthesized using four different mixing methods

3.2 Effects of Mixing Parameters on Density

Results have shown the link between some mixing parameters and the final density of NBT ceramics, presented in Figure 3. NBT2 possessed the greatest density and NBT3 the least. The higher density of NBT2 is related to its longer mixing time (5 h), faster mixing speed (500 rpm), and further ball milling, which promoted the precipitation between particles and better homogeneity of the sample. In contrast with NBT3 and NBT4, the shorter mixing time under a lower level of intensity promoted larger (i.e., less uniform) particle size distributions that led to a decrease in densification for both glasses. During sintering, the ineffective reorientation of particles distributed in the sintering reduces its universal density [19]. This poor particle mixing is associated with a lower mixing energy for low speed of rotation, and reduced structural integrity at select higher speeds. It has also been observed during milling scores using time to modulate parameters that can even be extended to mixing times in order to obtain high-density NBT-based ceramics.

3.3 Correlation Between Processing, Structure, and Properties

The direct correlation between XRD and the dielectric properties of the samples. For such characteristic rhombohedral reflections, more samples with stronger polarization tendency will generally have larger peak intensities. This suggests that the increased crystallinity from better mixing is positive for the well-aligned ferroelectric domain structure. The increased intensity and sharper diffraction peaks indicate a more ordered and stable structure. For well-mixed samples like the NBT2, the absence of secondary phases clearly showed that enough energy for mixing seemed to have a positive effect on complete solid-state reactions. Additionally, loss of bismuth can be minimized, as is illustrated in Figure 2.

3.4 Implications for Processing Optimization

These results demonstrate that the rhombohedral phase of NBT is unreactive to processing conditions. However, the quality of the crystal (as measured by powdered XRD peaks shape and intensity) is susceptible to mixing. This indicates that an improvement of the mixing and thermal treatments is more important for improving the structure and dielectric properties of NBT, rather than adaptations on post-processing.

3.5 Dielectric Permittivity Analysis in NBT-Based Ceramic Systems

The temperature dependence of the dielectric data in Figure 4 and Table 3 presents important information that is relevant to the $Na_{0.5}Bi_{0.5}TiO_3$ (NBT) ceramics by two means of mixing. A correlation between processing conditions and characteristic ferroelectric-to-paraelectric phase transition in the dielectric constant vs. temperature plot is seen at 1kHz.

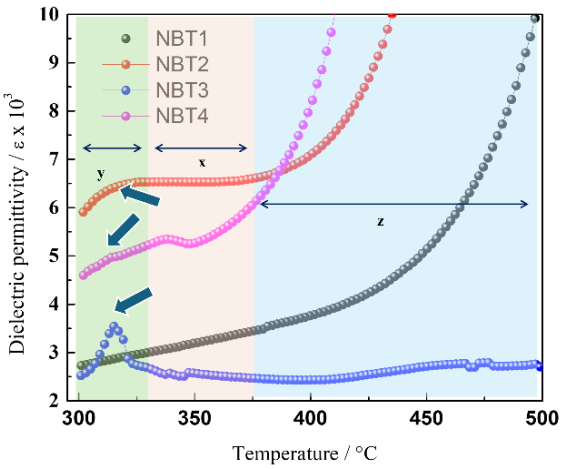

Figure 4 Dielectric permittivity versus temperature

Table 3 Dielectric permittivity of NBT samples measured at chosen temperatures

Sample	Temperature, °C / Dielectric permittivity, ε		
	300	Tm_1	500
NBT1 (No Ball Milling)	2727.41	10680.37 at 500 °C	10680.37
NBT2 (Mixing and Milling)	5905.76	6534.04 at 336.21 °C	57150.30
NBT3 (Moderate Mixing and Milling)	2522.89	3542.01 at 315.12 °C	2722.28
NBT4 (Short-Intensity Mixing)	4599.511	5336.78 at 340.21 °C	99779.62

In Region Y, a broad peak of moderate intensity is observed for the sample NBT1 (green curve). This less distinct peak in dielectric results could be explained by localized field and polarization variations due to inhomogeneities in microstructure [20]. Furthermore, the absence of typical phases or the local defects can hinder us from observing phase transitions in NBT1 [9]. This supports some earlier results [13];[40] that structural disorder, such as cation disorder or symmetry reduction, weakens the dielectric peaks. Although the process is kept the same, features in terms of environment, such as defect distribution and phase uniformity, may overwhelm those of the dielectric way [6].

The peak-broadening factor margin in NBT 2 is larger than that in Region NBT 1, unlike the dielectric-anomaly-containing factor margin. This suggests that, although the mixing is driven further by milling, at least some compositional or structural disorder persists. The development (evolution, disorder) has not been mapped out stage by stage, but it does establish a condition for an alternative spontaneous transition from ferroelectric to paraelectric.

From all the samples, NBT 3 appears to have the highest strength of peaks, indicating superior mixing and thermal conditions at a given phase purity. These results are in agreement with three-dimensional numerical simulations, which were reported by Li *et al*. (2023). A stronger peak can also be considered to result from enhanced mixing of components, supporting global ferroelectric domains and lower local inhomogeneity effects [34]. This enhanced uniformity results in a more predictable and consistent dielectric response. This stability is demonstrated by the sharper peak (a clear phase transition) for enhanced energy storage [8];[24]. The homogeneity of the material is likely to be due to well-mixed precursors during synthesis and applied thermal conditions [42].

NBT 4 is described as being calcined for seven hours, and the remixer time of this is lower than that of all other samples. NBT 4's dielectric response indicates a wider, but less pronounced peak. Shortened mixing times result in more voids in the structure being produced, which adversely impairs dielectric performance, and therefore leads to an imbalance between structures modelled.

Overmixing, and (in this case) over calcination, and a slightly lower dip in temperature and sintering at about 1100°C, result in structural inhomogeneities and more random grain growth, further widening the ferro-to paraelectric transition spectrum. These particular settings could be responsible for the lack of quality of the phases and poor interdomain uniformity, thus diminishing and broadening the dielectric anomaly at (Tm). Moreover, the lower temperature sintering may also be helpful in fabricating stoichiometric NBT ceramics and in avoiding any sort of volatilization/ evaporation that may result from excessive heating [15].

Interestingly, the sharp and clear peak is similar to the results of Mesrar *et al*. [25], who reported that optimal processing gave a strong dielectric anomaly at T_c because of effective mixing and high phase purity. In region X displays the dielectric constant exhibits a clear transition for all sample, though the peak is less sharp compared to Region Y [17]. This implies that there could be mixing parameter and preparation condition (e.g., mixing time, calcination period) downfalls, which lead to nonuniformity of the phase and published clarity or no anomaly at Tc.

Region Z exhibits a sudden decrease of the dielectric constant at the Tm maximum, as is also typical for paraelectric contribution in the transformation from ferroelectric to non-ferroelectric region in the phase diagram. This decrease involves the process condition and dielectric micro stability phase of NBT as well. In Z, the dielectric constant itself of NBT 1 falls faster than in some parts of the structural inhomogeneity, indicating early paraelectricity. As a result, a smaller drop in NBT 2 (compared to the case of NBT 1) is observed here, which may be related to the enhancement of phase uniformity so that it

stretches the starting point for paraelectric behavior further. On the other hand, NBT 3 has a more moderate inside a Region Z, in which the enhanced dielectric constant persists at an enlarged temperature. This behavior is attributed to a higher sample phase purity and better mixing and thermal processing. NBT4 exhibits an even sharper decrease of dielectric constant below Tm within Region Z. Those processing conditions are such that the continuity of ferroelectric domains is disrupted, resulting in structural inhomogeneities which facilitate a very unusual sharp paraelectric transition.

The dielectric peak feature can be exposed in several ways. For those we mentioned above, one can include the degree of mixing. The optimal mixing factor is that after which the phases are largely not uniform. Poor mixing leads to compositional gradients or disordered domains, which then widen across the transition.

It has been observed in all investigations on NBT-based ceramics that, besides a disordered and inhomogeneous structure, plays an important role for dielectric properties and relaxor behavior [7];[18]. Poor mixing leads to mixed-grain populations in specimens, dominated by a kind of dominant grain that influences the electrical behavior through favored conduction routes [43]. The support information indicates that homogeneous mixing is the most important factor for obtaining the desired functional properties.

Phase concentration and homogeneity, among others, are also related to a certain extent. NBT 3 still has a high degree of phase concentration, which, in part, is necessary within reasonable limits for the presence of a significant and well-defined dielectric anomaly. On this condition, any departure from it can smear the peak for some reason. A huge amount of recent literature describes phase purity and dielectric anomalies as related phenomena. Both the PNRs and some structural disorder cause a significant modification of dielectric properties. This is even truer for dielectric anomalies sharpness [1]. Furthermore, in NBT relaxors, [20] emphasized the harmful impact of chemical inhomogeneities on dielectric properties. Phase purity was also highlighted in the literature with regard to optimal dielectric properties.

Boundaries of grains and defect structures always appear as similarly important ingredients. Relics of ferroelectric order, along with the destabilizer's microstructural defects, local non-stoichiometry, and grain boundaries, give rise to the broadening seen in NBT 1, NBT 2, as well as NBT 4. In particular, the chemical inhomogeneity (non-uniform distribution of oxygen vacancies) has a significant influence on the electrical and ferroelectric properties of NBT-based ceramics. This thereby helps in core-shell formation, which is essential to make low residual P–E hysteresis curves. Moreover, the nanomorphology of the negative enhanced the ferroelectricity behavior of the material at room temperature, clearly observed from higher polarization and lesser hysteresis compared to the positive. This will be useful for energy storage and piezoelectric devices [15]. The structural difference makes the dielectric responses wider through the local polarization mismatch near grain boundaries and defects [20].

Furthermore, it is highlighted that the dielectric and piezoelectric properties are influenced by the coexistence of ferroelectric phases and the effects of chemical inhomogeneity. Defects and grain boundaries break up the ferroelectric order. This makes the phase transition more spread out and the dielectric peaks broader.

The mixing and heating conditions really matter for how these NBT ceramics work. Looking at regions X, Y, and Z, we see that getting the right mixing speed, time, and temperature is crucial for clean phases and sharp transitions. When these aren't right (like in the other samples), the transitions get messy and the dielectric response drops.

NBT3 has a clear dielectric peak at about 320°C, just like Singh *et al*. found in 2023 [37]. The peak hits around 3500 for the dielectric constant. This matches what Vijayeta *et al*. reported for pure NBT back in 2014, so our processing worked well to get clean, uniform material.

NBT4 and NBT2 only show weak bumps around 320°C. The transition is still there but much weaker than NBT3. This probably comes from uneven microstructure, more defects, or extra phases - either from not mixing long enough (NBT4) or poor heat treatment (NBT2).

NBT1 was made without ball milling, just heated to 50°C. Its dielectric transition is pretty weak. Without the ball milling, the starting materials don't mix well, so you get uneven composition or incomplete reactions. That's why it looks so different from the well-processed NBT3.

The processing really controls how these materials behave. NBT3 works best because we got the mixing and heating just right for clean phases and good dielectric properties. The other samples (NBT1, NBT2, NBT4) had processing problems that created defects and hurt their properties. This presents how essential it is to control processing when making high-performance ferroelectric materials [14]. NBT3's sharp peak looks a lot like what Mesrar *et al*. saw in 2020 they also got clean dielectric behavior when they processed their ceramics properly.

According to our examination, the dielectric peak of NBT3 is also similar to that observed after processing operation, which means that the same preparation scheme not only leads to a macroscopic enhancement in the dielectric response but also an associated generic signature in the phase transition behavior. That shows the mixing parameters extracted from the literature can be fine-tuned to recover the intrinsic dielectric response of these NBT ceramics.

3.6 AC Dielectric Permittivity Analysis in NBT-Based Ceramic Systems

The module of the dielectric permittivity (ε') is shown in Figure 5 (a) and (b), respectively, against their respective frequencies (100 Hz to 1 MHz) for all NBT samples.

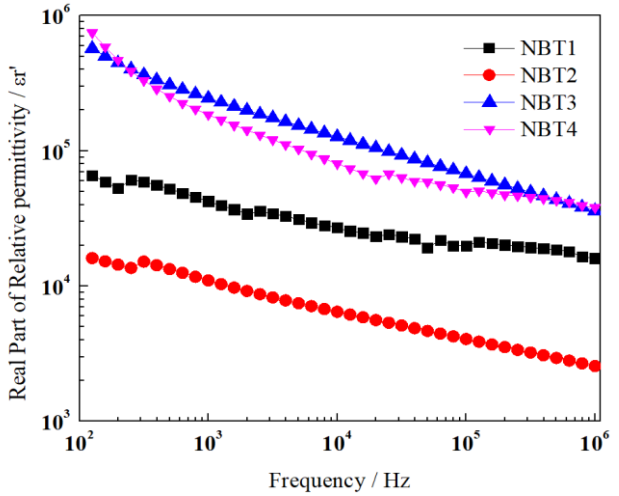

Figure 5 (a) Real part of relative permittivity versus frequency

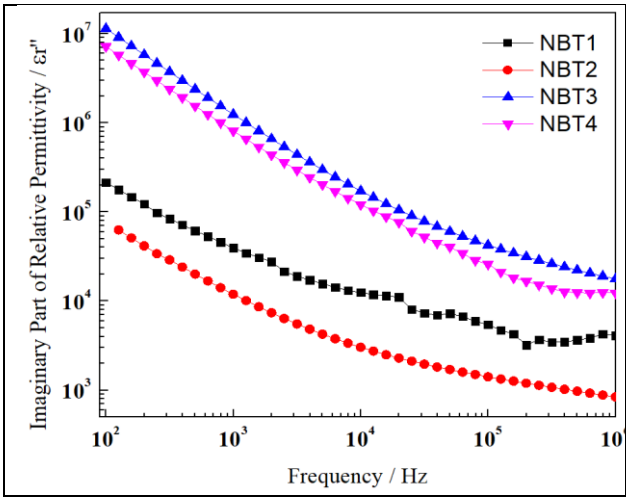

Figure 5 (b) Imaginary part of relative permittivity versus frequency

This behavior was attributed to dielectric relaxation processes, polarization mechanisms that behave differently depending on the frequency range. The dielectric constant changes based on things like how fast the electric field switches and what the material looks like inside. When the frequency goes up, ε' usually drops because the slower polarization types (like dipolar or ionic) can't keep up with the fast-changing field. This gives you a lower dielectric constant [45].

NBT-3 works so well because we got the processing just right. The calcination time reached the optimal point because of having enough time to form proper phases without creating excess defects. Good mixing distributed the Na^{+}, Bi^{3+}, and Ti^{4+} ions uniformly, leading to better ferroelectric domain organization. Using methods like sol-gel or hydrothermal synthesis helps a lot with this because you can control the chemistry better and get the ions mixed properly [39].

The sintering temperature and time for NBT-3 let the grains grow to the right size and packed everything together well. This cut down on pores and made better grain boundaries. The processing also kept oxygen vacancies low, which is good because these defects mess up the ferroelectric order in perovskite materials.

The lower density in NBT-3 actually helps instead of hurts. The pores are probably isolated and spread out evenly, not connected to each other. They're tiny and sit at grain boundaries where they create helpful stress that makes domain walls move easier.

This lower density structure lets domain walls move around more freely. It cuts down on the internal stress that usually stops domains from switching direction. This gives the ferroelectric domains more space to respond when you apply an electric field, so you get bigger polarization because there's less mechanical resistance. This makes sense because domain wall movement is key for getting good piezoelectric and dielectric behavior in ferroelectric materials [33].

The way we processed NBT-3 probably gave us a good distribution of oxygen vacancies. These vacancies can actually boost polarization by making defect dipoles that line up with the spontaneous polarization instead of fighting it. The more relaxed lattice structure from having the right amount of oxygen vacancies lets the ions move further, which helps the ferroelectric properties even more. This fits with what Li *et al*. [20] - that changing oxygen vacancy levels really affects how NBT-based ceramics behave electrically.

Despite lower density, NBT-3 may have a more ideal rhombohedral-to-tetragonal phase ratio at the morphotropic phase boundary, enhanced phase coherence at interfaces that amplifies the overall polarization, and better chemical homogeneity within grains, even with more porous grain boundaries. NBT-3 has better chemical mixing within its grains, which makes it work better. When elements and phases spread out evenly, you get less internal stress and fewer defects, so the electrical properties stay more stable. Getting this even mixing matters a lot for piezoelectric materials because uneven spots cause performance problems [35].

The slightly lower but still impressive dielectric response of NBT-4. A 7-hour calcination may have facilitated the achievement of a good phase purity, though, possibly at the expense of some slight structural strain or minor compositional variations. The sintering temperature of 1099°C will ensure good densification, but probably at the cost of bismuth volatilization compared to NBT-3. This resulted in A-site vacancies that weakened the polarization response. The 1-hour mixing period was sufficient to provide a homogeneity that was, however, lower than NBT-3.

The moderate dielectric response of NBT-1 hints at the processing to be less than ideal for phase formation. Perhaps inadequate calcination time or temperature resulted in a partial formation of phases or secondary phases. It can speculate that the sintering conditions achieved a positive but not ideal grain size and morphology, leading to an increased concentration of grain boundaries, which hamper the motion of domain walls. A higher concentration of point defects and oxygen vacancies, where domain walls can be pinned, also results in lowering the ability to polarize systems.

A much smaller dielectric response of NBT-2 signifies high processing conditions that favoured densification effects. High-temperature action is usually required for high-density processing, with some resulting in Bi loss. This loss, in turn, leads to A-site vacancies within the perovskite and would disrupt the required polarization for the best dielectric characteristics. The overall polarization when a field is applied externally remains poor, too, because of vacancies that suppress the dielectric response [30];[10]. In addition, the absence of bismuth results in internal stresses that might pin the domain walls and hence lower the polarization. According to [11], the impossibility for domain walls to move freely results in a larger stored energy [41]. The densification may have induced abnormal grain growth that results in different granule size distributions, the formation of grain boundary phases with low permittivity, which significantly controls the total response and the pinning of defects by defects at grain boundaries. Abnormal grain growth with different sizes of grains may occur during densification. These phenomena may have a strong influence on the electro-physical properties of the material, as in many cases larger grains dominate the dielectric response, whereas smaller grains play almost a negligible role [34]. Besides that, the dielectric response could be strongly influenced by the low-permittivity region on grain boundaries. Such sections are generally known to impede charge transport and thereby lower the effective dielectric constant of the ceramic. Their formation is often attributed to the processing parameters and the chemical makeup of the material [2].

The high-density processing may have induced the deviation from the ideal Na:Bi stoichiometry due to differential volatilization, the reduction of A-site disorder that is actually beneficial for NBT's relaxor-like behaviour, and oxygen over-stoichiometry that diminishes the concentration of beneficial oxygen vacancies [38].

The highly dense structure may reduce lattice flexibility that limits the polarization response, stronger coupling between neighboring dipoles that increases the energy barrier for polarization switching, and diminished contribution from extrinsic mechanisms (domain wall motion) to the overall dielectric response. Together, these factors affect the dielectric properties of the material, especially for energy storage applications [2]. Inadequate mixing or calcination parameters that lead to compositional fluctuations and increased disorder in the crystal structure. Secondary phases from poor mixing or wrong thermal treatment can complicate the crystal structure [26]; [29]. It also supported by another study [3]. Among the various process conditions generating a defect complex detrimental to long range order of ferroelectricity (and hence of polarizability) can be vacancies and interstitials, which introduce local lattice distortions [20]. Where bismuth is lost at high processing temperatures, and if they are uncontrolled or unaccounted for losses during processing, A-site vacancies do become a harsh reality in gross ferroelectricity weakening.

These vacancies can aggravate the problem by weakening and destabilizing the ferroelectric phase, which is not favorable for energy storage and electrocaloric applications of the material [4]. This disorder and compositional fluctuation effect plays a crucial role in the dielectric, ferroelectric behaviour of NBT-based deriva-tives.

On the log-log plot, the slope of ε' vs frequency shows more useful information about dynamic dielectric relaxation. Higher slopes indicate a pronounced frequency dependence, corresponding to broad retarded relaxation time distributions. This distribution is consistent with the coexistence of several polarization mechanisms (electronic, ionic, as well as interfacial) having different timescales of relaxation. Such conditions, however, may be modified based on such factors as the particle sizes, sintering, and defect levels. The slope of the curve ε' versus frequency provides additional information for dielectric relaxation; increasing this slope shows an increase in the range of relaxation times, and several mechanisms are present. One similar observation was presented, and also confirmed our observation that the dielectric behavior essentially scales with how processing conditions interplay [12]. The consistent trends across all samples in Figure 6 and Table 4 also confirm the reliability of these results.

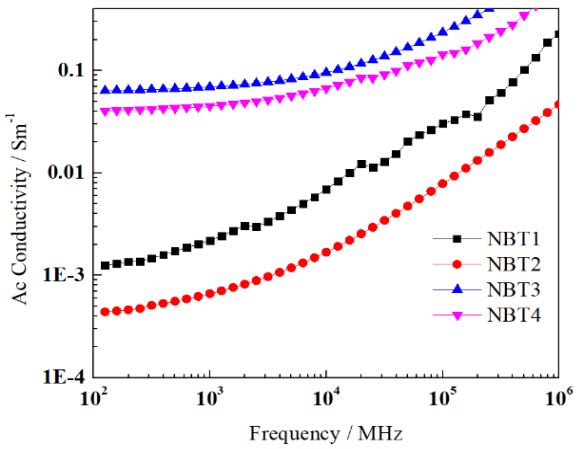

Figure 6 Ac conductivity versus frequency

Table 4 Electrical conductivity of NBT samples measured at various frequencies

Frekuency (Hz)	NBT1	NBT2	NBT3	NBT4
1,000,000	0.22821	0.04674	0.98197	0.68717
99,998	0.03026	0.00785	0.23577	0.14406
9,999	0.00694	0.00168	0.09567	0.06705
999	0.00219	0.00066	0.06913	0.04505

NBT-1 shows an intermediate level of AC conductivity. Its curve follows a moderate increase with frequency, a typical trend for hopping or localized charge transport. Although its conductivity values are not the highest among the samples, the steady slope suggests that the conduction mechanism is neither strongly activated nor heavily suppressed by processing-induced defects.

The red curve for NBT-2 displays the lowest AC conductivity values across the measured frequency range. This indicates that the conduction pathways are not well established in this sample. Higher density or processing that yields a locked microstructure likely constrains charge-carrier mobility and suppresses the frequency response [21]. Greater densification also constrains carrier motion and lowers conductivity [23].

The blue line representing NBT-3 is the highest among the curves. Its values are significantly higher at all frequencies, suggesting enhanced hopping or a more effective conduction network [15]. This implies that the processing conditions for NBT-3 have created a structure (possibly with more optimally distributed defects or favorable grain boundary characteristics) that facilitates charge carrier movement.

NBT-4 exhibits the second-highest AC conductivity (by being just below NBT-3). The curve shows that although it follows a similar trend with frequency, its conductivity values are slightly lower than those of NBT-3. This may indicate that while its microstructure and defect configuration support charge transport, they are not as ideal as that of NBT-3 for maximizing conduction.

In summary, these differences emphasize how processing conditions can dramatically alter the conduction network within the material. Each sample shows distinct dielectric and conductivity characteristics, with NBT2 exhibiting the lowest conductivity and high permittivity at elevated temperatures, indicating promising potential for dielectric applications. The comparative analysis suggests that NBT2 may offer a favourable balance between low conductivity and high-temperature dielectric performance.

3.7 AC Dielectric Permittivity Analysis in NBT-Based Ceramic Systems

Figure 7 shows how tan δ changes with frequency for the four NBT samples. tan δ value drops sharply as frequency goes up because dipolar relaxations can't follow the fast-switching field [22]. Higher frequencies give lower dielectric loss values. This happens because low frequencies let all polarization types work together, but high frequencies only allow electronic polarization to respond [27].

NBT3 (mixed and milled at room temperature) has the highest dielectric loss at low frequencies. This points to major polarization losses from more defects and grain boundary problems that cause space charge buildup and interfacial polarization [31]. NBT2 (also mixed and milled at room temperature) shows the lowest loss because it formed a dense structure with fewer defects, so less energy gets wasted during use [34]. NBT1 and NBT4 fall somewhere in between.

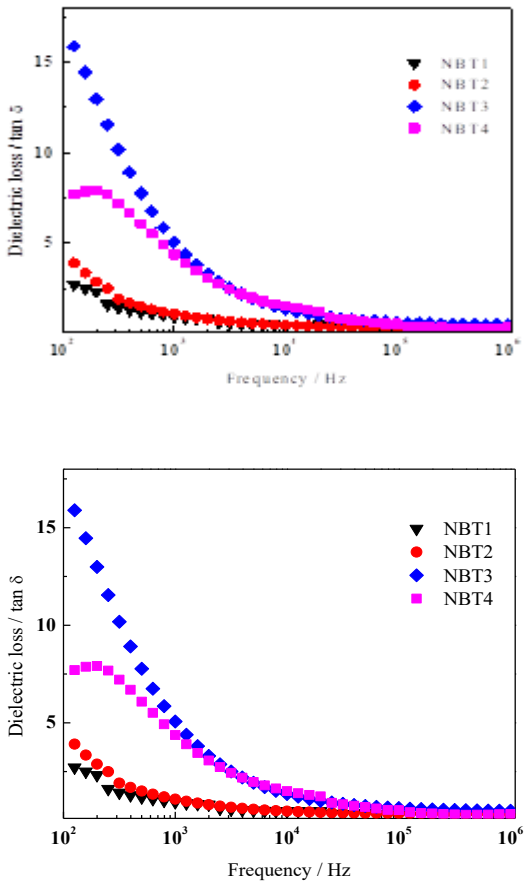

Figure 7 Dielectric loss versus frequency

These differences also account for its superior dielectric properties, including a high dielectric constant of 3250 at room temperature (1 kHz) and an almost constant Curie temperature of 320°C.

Results indicate that better mixing homogeneity decreases both bismuth loss and secondary phase formation, enhancing the performance of NBT ceramic. The relationship between processing, microstructure, and properties also provides useful insights into the design of high-performance lead-free ferroelectrics. These materials can be used in sensors, actuators, and energy storage, supporting the global shift toward alternatives to lead-based electronics.

The impact of processing routes on the microstructure and, hence, the dielectric performance of the NBT ceramics. At low frequencies, the dielectric loss factor shows dispersion, but the values drop at higher frequencies. This reflects a shift from weakly conducting grain boundaries to strongly conducting grains [37]. The loss decreases as frequency rises, showing that polarization mechanisms like dipolar and space charge are less effective at higher frequencies [5].

4.0 CONCLUSION

This study characterized the influence of various mixing parameters on the structural and dielectric properties of $Na_{0.5}Bi_{0.5}TiO_3$ (NBT) ceramics. All samples exhibited a rhombohedral perovskite structure (space group R3c), as confirmed by XRD. Differences in peak sharpness indicated variations in crystallinity and structural order, reflecting the impact of processing on phase formation. Dielectric measurements revealed distinct permittivity values and transition temperatures among the samples, while AC conductivity analysis highlighted different conduction behaviors. Although no microstructural characterization was performed, prior studies suggest that improved mixing may reduce bismuth loss and minimize secondary phase formation, thereby enhancing material performance. These findings underline the critical role of processing in tailoring the physical properties of lead-free ferroelectric ceramics and offer useful insight for future applications in sensors, actuators, and capacitors.

Acknowledgement

The authors would like to thank Universiti Kuala Lumpur (UniKL) for the financial support under the Article Processing Charge (APC) grant and Universiti Kebangsaan Malaysia (UKM) for the providing lab facilities to support this research. This work was also supported by the Ministry of Higher Education Malaysia and the Graduate Excellence Programme (GrEP) funded by Majlis Amanah Rakyat (MARA). This work was supported by funding by the Ministry of Higher Education Malaysia.

Conflicts of Interest

The authors declare that there is no conflict of interest regarding the publication of this paper.

References

[1] Aissa, M., M. A. Slimani, A. Dhahri, M. Rasheed, Z. Raddaoui, S. E. Kossi, *et al.* 2022. Multifunctionality of Rare Earth Doped 0.925 Na0.5Bi0.5TiO3–0.075 K0.5Na0.5NbO3 Ferroelectric Ceramics. *Journal of Alloys and Compounds.* 921: 166188.

[2] Ancy, G. C., L. Venkidu, P. M. P. Dharsini, D. Dayanithi, N. V. Giridharan, and B. Sundarakannan. 2023. Temperature-Dependent Energy Storage Performance of the Ceramics in MPB Region Identified from the (1−(x+y))(Bi0.5Na0.5)TiO3-xBaTiO3-yBaZrO3 Ternary Ceramics. *Journal of Materials Science: Materials in Electronics.* 34(17): 1373. https://doi.org/10.1007/s10854-023-10799-8.

[3] Azlan, U. A. A., W. Krengvirat, A. F. M. Noor, K. A. Razak, and S. Sreekantan. 2012. Sintering and Characterization of Rare Earth Doped Bismuth Titanate Ceramics Prepared by Soft Combustion Synthesis. In *Sintering of Ceramics—New Emerging Techniques*. Winchester. InTech.

[4] Benyoussef, M., M. Zannen, C. Bouzidi, K. Taibi, H. Belmabrouk, S. Alaya, and J. Dhahri. 2021. Structural, Dielectric, and Ferroelectric Properties of Na0.5(Bi1-xNdx)0.5TiO3 Ceramics for Energy Storage and Electrocaloric Applications. *Ceramics International.* 47(18): 26539–51.

[5] Benyoussef, M., M. Zannen, C. Bouzidi, K. Taibi, H. Belmabrouk, S. Alaya, and J. Dhahri. 2018. Dielectric, Ferroelectric, and Energy Storage Properties in Dysprosium Doped Sodium Bismuth Titanate Ceramics. *Ceramics International.* 44(16): 19451–60. https://doi.org/10.1016/j.ceramint.2018.07.182.

[6] Bi, N., W. G. Wang, X. Y. Li, T. Liu, and G. L. Hao. 2018. The Effect of Dual Substitution of Na and Al on Ionic Conductivity. *Results in Physics.* 11: 422–26. https://doi.org/10.1016/j.rinp.2018.09.028.

[7] Bikse, L., E. Platacis, M. Antonova, A. Sternberg, and A. Kalvane. 2021. Impact of Thermal Treatment on the Surface of Na0.5Bi0.5TiO3-Based Ceramics. *Crystals.* 11(10): 1266. https://doi.org/10.3390/cryst11101266.

[8] Cui, C., Y. Wang, B. Li, L. Zhang, H. Du, D. Zhou, *et al.* 2017. Structure, Dielectric and Relaxor Properties in Lead-Free ST-NBT Ceramics for High Energy Storage Applications. *Journal of Alloys and Compounds.* 711: 319–26.

[9] Dawson, J. A., H. Chen, and I. Tanaka. 2015. Crystal Structure, Defect Chemistry and Oxygen Ion Transport of the Ferroelectric Perovskite, Na0.5Bi0.5TiO3: Insights from First-Principles Calculations. *Journal of Materials Chemistry A.* 3(32): 16574–82. https://doi.org/10.1039/C5TA03705K.

[10] Diaz, J. C. C. A., J.-C. M'peko, M. Venet, and P. S. da Silva. 2020. Unveiling the High-Temperature Dielectric Response of Bi0.5Na0.5TiO3. *Scientific Reports.* 10(1): 19491.

[11] Fancher, C. M., S. Brewer, C. C. Chung, S. Röhrig, T. Rojac, G. Esteves, *et al.* 2017. The Contribution of 180° Domain Wall Motion to Dielectric Properties Quantified from In Situ X-Ray Diffraction. *Acta Materialia.* 126: 36–43. https://doi.org/10.1016/j.actamat.2016.12.037.

[12] França, E., P. Romanholo, S. Simões, E. Falcão, A. Franco Jr., and F. Machado. 2021. Enhancing the Electrical Properties of NBT Ceramics by the Addition of Small Amounts of Yb. *Journal of Alloys and Compounds.* 873: 159845.

[13] Feng, W., B. Luo, S. Bian, E. Tian, Z. Zhang, A. Kursumovic, J. L. MacManus-Driscoll, X. Wang, and L. Li. 2022. Heterostrain-Enabled Ultrahigh Electrostrain in Lead-Free Piezoelectric. *Nature Communications.* 13(1): 5086.

[14] Goutham, C., S. Raavi, and S. Asthana. 2019. Particle Size Dependent Properties of Na0.5Bi0.5TiO3 Synthesized Using Hydrothermal Technique. https://doi.org/10.1063/1.5093828.

[15] Jayasri, S., P. Elorika, and S. Anwar. 2023. Effect of Sintering Time on Electrical, Ferroelectric, and Piezoelectric Performances of Microwave Synthesized Sodium Bismuth Titanate Ceramics. *Materials Science and Engineering B.* 298: 116823.

[16] Khan, I. H., M. S. Habib, A. Maqbool, M. A. Rafiq, A. Ali, K. Nur, *et al.* 2024. Comparative Analysis of Bulk Ceramics and Thick Film Coatings for Optimized Energy Storage Technologies. *Scientific Reports.* 14(1): 31800.

[17] Kuanar, B., H. Mohanty, B. Dalai, and D. Behera. 2022. Structural and Electrical Properties of Bismuth Sodium Titanate Ceramic. In *IOP Conference Series: Materials Science and Engineering.* 1258(1): 012007.

[18] Kuanar, B., B. Dalai, D. Behera, and H. S. Mohanty. 2023. Impact of Gd3+ Substitution on the Structural, Morphological, and Electrical Properties of Lead-Free Bi0.5Na0.5TiO3 Ceramics. *Journal of Materials Science: Materials in Electronics.* 34(6): 506.

[19] Li, Y., H. Chen, Y. Wang, H. Du, J. Shi, X. Liu, *et al.* 2020. Improved Electric Energy Storage Properties of BT-SBT Lead-Free Ceramics Incorporating A-Site Substitution with Na and Bi Ions and Liquid Sintering Generated by Na0.5Bi0.5TiO3. *Journal of Alloys and Compounds.* 156708. https://doi.org/10.1016/j.jallcom.2020.156708.

[20] Li, Y., R. Rao, Y. Wang, H. Du, J. Shi, and X. Liu. 2023. Effect of Chemical Inhomogeneity on the Dielectric and Impedance Behaviors of Bismuth Sodium Titanate Based

Relaxors. *ECS Journal of Solid State Science and Technology*. 12(1): 013005.
[21] Li, M., Q. Xu, C. Zhu, W. Luo, Y. Gu, X. Wang, *et al.* 2021. Investigation of Ga Doping for Non-Stoichiometric Sodium Bismuth Titanate Ceramics. *Journal of Materials Science: Materials in Electronics*. 32: 16104–12.
[22] Madolappa, S., H. K. Choudhary, N. Punia, A. V. Anupama, and B. Sahoo. 2021. Dielectric Properties of A-Site Mn-Doped Bismuth Sodium Titanate Perovskite: (Bi0.5Na0.5)0.9Mn0.1TiO3. *Materials Chemistry and Physics*. 270: 124849. https://doi.org/10.1016/j.matchemphys.2021.124849.
[23] Malathi, A. R., G. S. Kumar, and G. Prasad. 2015. Effect of SrTiO3 on Dielectric and Piezoelectric Properties of NBT. *Phase Transitions*. 88(2): 169–82. https://doi.org/10.1080/01411594.2014.964715.
[24] Mesrar, M., A. Elbasset, N.-S. Echatoui, F. Abdi, and T. Lamcharfi. 2022. Studies of Structural, Dielectric, and Impedance Spectroscopy of KBT-Modified Sodium Bismuth Titanate Lead-Free Ceramics. *ACS Omega*. 7(42): 37142–63. https://doi.org/10.1021/acsomega.2c03139.
[25] Mesrar, M., T. Lamcharfi, N. S. Echatoui, and F. Abdi. 2022. Effect of Sintering Temperature on the Microstructure and Electrical Properties of Na0.5Bi0.5TiO3 Processed by the Sol–Gel Method. *Journal of Sol-Gel Science and Technology*. 103 (3): 820–31. https://doi.org/10.1007/s10971-022-05885-y.
[26] Nakonieczny, D. S., F. Kern, L. Dufner, A. Dubiel, M. Antonowicz, and K. Matus. 2021. Effect of Calcination Temperature on the Phase Composition, Morphology, and Thermal Properties of ZrO2 and Al2O3 Modified with APTES (3-Aminopropyltriethoxysilane). *Materials*. 14(21): 6651.
[27] Niu, X., X. Jian, X. Chen, H. Li, W. Liang, J. Chen, *et al.* 2023. Superior Energy Storage Properties in Lead-Free Na0.5Bi0.5TiO3-Based Relaxor Ferroelectric Ceramics via Compositional Tailoring and Bandgap Engineering. *Scripta Materialia*. 230: 115387.
[28] Pal, V., R. Dwivedi, and O. Thakur. 2014. Effect of Neodymium Substitution on Structural and Ferroelectric Properties of BNT Ceramics. *Materials Research Bulletin*. 51: 189–96.
[29] Pascual, M. N.-L., E. M. Moreno, L. O. Jøsang, M. Merlo, and J. J. Biendicho. 2024. Revealing the Impact of CO2 Exposure During Calcination on the Physicochemical and Electrochemical Properties of LiNi0.8Co0.1Mn0.1O2. *Nanoscale*. 16(48): 22326–36.
[30] Paterson, A. R., H. Nagata, X. Tan, J. E. Daniels, M. Hinterstein, R. Ranjan, *et al.* 2018. Relaxor-Ferroelectric Transitions: Sodium Bismuth Titanate Derivatives. *MRS Bulletin*. 43 (8): 600–606.
[31] Ren, P., Z. Wang, N. Sun, P. Zhao, Y. Liu, Y. Guo, *et al.* 2021. High Field Electroformation of Sodium Bismuth Titanate and Its Solid Solutions with Barium Titanate. *Journal of Materials Chemistry C*. 9(9): 3334–42. https://doi.org/10.1039/D0TC05728B.
[32] Rhimi, N., N. Dhahri, M. Khelifi, E. Hlil, and J. Dhahri. 2022. Structural, Morphological, Optical and Dielectric Properties of Sodium Bismuth Titanate Ceramics. *Inorganic Chemistry Communications*. 146: 110119.
[33] Riess, K., N. H. Khansur, A. Martin, A. Benčan, H. Uršič, and K. G. Webber. 2021. Stress- and Frequency-Dependent Properties of Relaxor-Like Sodium Bismuth Titanate. *Physical Review B*. 103(9): 094113. https://doi.org/10.1103/PhysRevB.103.094113.
[34] Sahu, R. K., and S. Asthana. 2024. Enhanced Energy Storage Performance, Breakdown Strength, and Thermal Stability in Compositionally Designed Relaxor Eu3+ Substituted Na0.2K0.3Bi0.5TiO3. *Journal of Energy Storage*. 91: 112020. https://doi.org/10.1016/j.est.2024.112020.
[35] Samantaray, K. S., A. Mishra, D. Rout, A. Srinivas, A. Perumal, and S. Sahoo. 2023. Room Temperature Magneto-Dielectric Coupling in the CaMnO3 Modified NBT Lead-Free Ceramics. *Applied Physics A*. 129(4): 237. https://doi.org/10.1007/s00339-023-06513-4.
[36] Shrout, T. R., and S. J. Zhang. 2007. Lead-Free Piezoelectric Ceramics: Alternatives for PZT? *Journal of Electroceramics*. 19(1): 113–26.
[37] Singh, S., A. Kaur, P. Kaur, and L. Singh. 2023. High-Temperature Dielectric Relaxation and Electric Conduction Mechanisms in a LaCoO3-Modified Na0.5Bi0.5TiO3 System. *ACS Omega*. 8(28): 25623–38.
[38] Steiner, S., J. Heldt, O. Sobol, W. Unger, and T. Frömling. 2021. Influence of Oxygen Vacancies on Core-Shell Formation in Solid Solutions of (Na,Bi)TiO3 and SrTiO3. *Journal of the American Ceramic Society*. 104(9): 4341–50.
[39] Takiul, I., S. Lee, and H. Hwang. 2024. Sinterability, Microstructural Evolution, and Dielectric Performance of Bismuth Sodium Titanate (Bi0.5Na0.5TiO3) Lead-Free Ferroelectric Ceramics. *Archives of Metallurgy and Materials*. 33–38.
[40] Viola, G., Y. Tian, C. Yu, Y. Tan, V. Koval, X. Wei, K.-L. Choy, and H. Yan. 2021. Electric Field-Induced Transformations in Bismuth Sodium Titanate-Based Materials. *Progress in Materials Science*. 122: 100837.
[41] Wang, Z., D. Xue, Y. Zhou, N. Wang, X. Ding, J. Sun, T. Lookman, and D. Xue. 2021. Enhanced Energy-Storage Density by Reversible Domain Switching in Acceptor-Doped Ferroelectrics. *Physical Review Applied*. 15(3): 034061.
[42] Wu, J., H. Wang, D. Su, G. Liu, B. Zhang, H. Du, *et al.* 2022. Enhanced Energy-Storage Performances in Sodium Bismuth Titanate-Based Relaxation Ferroelectric Ceramics with Optimized Polarization by Tuning Sintering Temperature. *Materials*. 15(14): 4981. https://doi.org/10.3390/ma15144981.
[43] Yang, F., M. Wu, Y. Huang, P. Li, W. Zhao, and S. Xu. 2020. From Insulator to Oxide-Ion Conductor by a Synergistic Effect from Defect Chemistry and Microstructure: Acceptor-Doped Bi-Excess Sodium Bismuth Titanate Na0.5Bi0.51TiO3.015. *Journal of Materials Chemistry A*. 8(47): 25120–30. https://doi.org/10.1039/D0TA10071D.
[44] Zhang, Y., X. Ke, K. Zhao, Z. Zhou, and R. Liang. 2022. Ca2+ Doping Effects on the Structural and Electrical Properties of Na0.5Bi4.5Ti4O15 Piezoceramics. *Ceramics International*. https://doi.org/10.1016/j.ceramint.2022.06.201.
[45] Zou, K., Y. Dan, H. Xu, Q. Zhang, Y. Lu, H. Huang, and Y. He. 2019. Recent Advances in Lead-Free Dielectric Materials for Energy Storage. *Materials Research Bulletin*. 113: 190–201.